
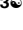

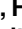

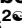


## RESEARCH ARTICLE

## Leaf water potential of coffee estimated by landsat-8 images

Daniel Andrade Maciel<sup>1</sup> , Vânia Aparecida Silva<sup>2†</sup>, Helena Maria Ramos Alves<sup>3</sup> , Margarete Marin Lordelo Volpato<sup>2†\*</sup> , João Paulo Rodrigues Alves de Barbosa<sup>4†</sup>, Vanessa Cristina Oliveira de Souza<sup>5†</sup>, Meline Oliveira Santos<sup>2</sup> , Helbert Rezende de Oliveira Silveira<sup>2</sup> , Mayara Fontes Dantas<sup>2†</sup>, Ana Flávia de Freitas<sup>2</sup> , Gladyston Rodrigues Carvalho<sup>2†</sup>, Jacqueline Oliveira dos Santos<sup>2†</sup>

**1** Pós-Graduação/Sensoriamento Remoto, Instituto Nacional de Pesquisas Espaciais, São José dos Campos, SP, Brasil, **2** Empresa de Pesquisa Agropecuária de Minas Gerais, Lavras, MG, Brazil, **3** Empresa Brasileira de Pesquisa Agropecuária, Brasília, DF, Brasil, **4** Dept. de Biologia, Universidade Federal Lavras, Lavras, MG, Brasil, **5** Instituto de Matemática e Computação, Universidade Federal de Itajubá, Itajubá, MG, Brasil

 These authors contributed equally to this work.

† These authors also contributed equally to this work.

\* [margarete@epamig.ufla.br](mailto:margarete@epamig.ufla.br)


 OPEN ACCESS

**Citation:** Maciel DA, Silva VA, Alves HMR, Volpato MML, Barbosa JPRAd, Souza VCod, et al. (2020) Leaf water potential of coffee estimated by landsat-8 images. PLoS ONE 15(3): e0230013. <https://doi.org/10.1371/journal.pone.0230013>

**Editor:** Elisabeth Bui, CSIRO, AUSTRALIA

**Received:** August 30, 2019

**Accepted:** February 19, 2020

**Published:** March 18, 2020

**Copyright:** © 2020 Maciel et al. This is an open access article distributed under the terms of the [Creative Commons Attribution License](https://creativecommons.org/licenses/by/4.0/), which permits unrestricted use, distribution, and reproduction in any medium, provided the original author and source are credited.

**Data Availability Statement:** All relevant data are within the paper and its Supporting Information files.

**Funding:** This work was supported by Consórcio Pesquisa Café #793.702/2013 under subprojects 02.13.02.050.00.00 (M.M.L.V), 02.13.02.049.00.03 and 02.13.02.050.00.02 (V.A.S), and 02.13.02.050.00.03 (H.M.R.A). V.A.S thanks Fundação de Amparo à Pesquisa do Estado de Minas Gerais (FAPEMIG) [BIP-00200-18/FAPEMIG]. D.A.M Ph.D. fellowship was supported by the Coordenação de Aperfeiçoamento de Pessoal de Nível Superior (CAPES) [001]. The

## Abstract

Traditionally, water conditions of coffee areas are monitored by measuring the leaf water potential ( $\Psi_w$ ) throughout a pressure pump. However, there is a demand for the development of technologies that can estimate large areas or regions. In this context, the objective of this study was to estimate the  $\Psi_w$  by surface reflectance values and vegetation indices obtained from the Landsat-8/OLI sensor in Minas Gerais—Brazil. Several algorithms using OLI bands and vegetation indexes were evaluated and from the correlation analysis, a quadratic algorithm that uses the Normalized Difference Vegetation Index (NDVI) performed better, with a correlation coefficient ( $R^2$ ) of 0.82. Leave-One-Out Cross-Validation (LOOCV) was performed to validate the models and the best results were for NDVI quadratic algorithm, presenting a Mean Absolute Percentage Error (MAPE) of 27.09% and an  $R^2$  of 0.85. Subsequently, the NDVI quadratic algorithm was applied to Landsat-8 images, aiming to spatialize the  $\Psi_w$  estimated in a representative area of regional coffee planting between September 2014 to July 2015. From the proposed algorithm, it was possible to estimate  $\Psi_w$  from Landsat-8/OLI imagery, contributing to drought monitoring in the coffee area leading to cost reduction to the producers.

## Introduction

In Brazil, coffee production has great economic and social importance, generating employment, and increasing the population's income. However, such production is threatened by extreme weather events, such as prolonged droughts and frost. Therefore, coffee plantations need to be constantly monitored in order to establish adequate management practices to minimize production losses. Traditionally, water conditions of coffee areas are monitored by

fundings had no role in study design, data collection and analysis, decision to publish, or preparation of the manuscript.

**Competing interests:** The authors have declared that no competing interests exist.

measuring the leaf water potential ( $\Psi_w$ ) through a pressure pump. However, measurement is time-consuming, involves high-cost equipment and maintenance, and is applicable only in small areas.

Monitoring the water conditions of coffee plantations requires the use of technologies that allow the evaluation of large areas or regions. In this context, the use of remote sensing presents as an opportunity to quantify drought stress when there is no in-situ weather station available (i.e., for time-series creation) [1,2]. In the past years, the new generation of free medium-resolution satellite imagery such as the Landsat-8/OLI and Sentinel-2/MSI presents suitable information for drought monitoring in agricultural lands [3,4]. Moreover, efforts such as the Harmonized Landsat and Sentinel-2 (HLS) to combine both satellites in a virtual constellation provide a seamless reflectance dataset with a reduced temporal resolution hence offering a high potential for crop monitoring [5].

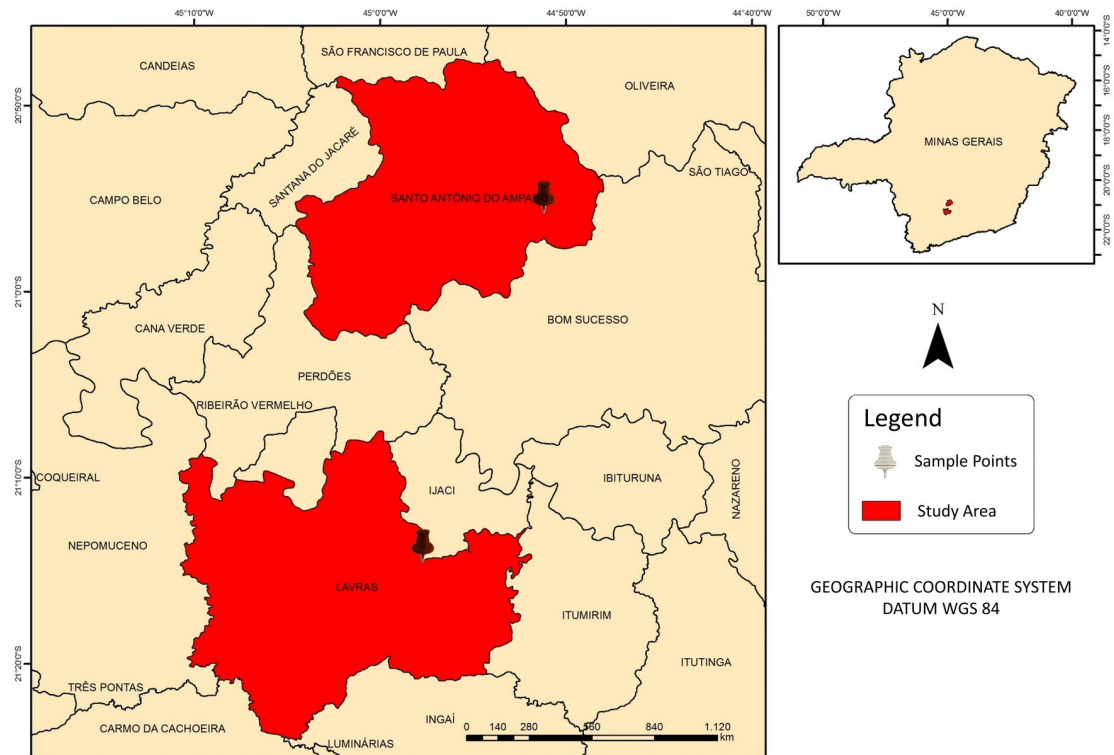
Recently, Ramoelo et al. [6] proposed modeling techniques to estimate the  $\Psi_w$  of crops using spectral data obtained by remote sensing using the RapidEye sensors. Furthermore, Chemura et al. [7] evaluated a model to estimate plant water content (PWC) in *Coffea arabica* based on field spectrometry. There are also vegetation indices that correlate well with biophysical vegetation parameters and are widely used in estimating biomass, changes in crop development, and are indicative of biotic and abiotic stress [7,8]. For example, the Normalized Difference Vegetation Index (NDVI) is one of the most commonly used vegetation indices in ecological studies as it provides a general measure of vegetation state [9,10]. As these biophysical parameters are related to climate variability [11], NDVI could be used as a surrogate measure of its variability [10,12]. Therefore, several works attempted to explore the relationship between NDVI and other vegetation indices (such as NDWI) with leaf water potential and water stress in different crop cultures. Pu et al. [13] evaluated oak leaves with different water concentrations and observed increased reflectance at wavelengths from 400 to 700 nm and decreased from 750 nm when submitted to water stress. Ramoelo et al. [6] found moderate values for the Pearson correlation between NDVI and  $\Psi_w$ , in dry seasons, using RapidEye images in South Africa, for different species of trees and pasture. As NDVI is sensitive to the presence of chlorophylls and other plant pigments that are responsible for the absorption of red band radiation [14], lower NDVI values under water deficit conditions indicate a decrease in chlorophyll concentration in leaves. Despite NDVI, another commonly used vegetation index for drought monitoring is the Normalized Difference Water Index (NDWI) [1,6,15].

Considering that  $\Psi_w$  is a precise parameter for measuring the water condition of the plant and that the spectral data obtained by remote sensing allows extensive area monitoring, models that establish a relationship between leaf water potential and remote sensing vegetation data that can be used as a monitoring technology of the water conditions of coffee plantations. Therefore, the objective of this study was to propose algorithms to estimate  $\Psi_w$  of coffee areas in Minas Gerais (Brazil) from remote sensing data. To address this objective, the following procedures were performed: i) *in-situ* measurements of  $\Psi_w$  were carried out between 2013–2017 over two cities in Minas Gerais state; ii) Landsat-8/OLI surface reflectance and vegetation indices were correlated with *in-situ*  $\Psi_w$ ; iii) Leave-One-Out-Cross-Validation (LOOCV) were used to obtain the performance and applicability of the algorithms; iv) Best algorithm was applied to Landsat-8/OLI imageries for spatialization.

## Materials and methods

### Study area

The study was conducted in experimental *Coffea arabica* variety Catuaí (spacing of 3,40 x 0,65 m) areas located in the municipalities of Santo Antônio do Amparo and Lavras (Fig 1). Both



**Fig 1. Study area.**

<https://doi.org/10.1371/journal.pone.0230013.g001>

cities are located in the south region of Minas Gerais, with an average altitude of approximately 950 m. According to the Köppen-Geiser climate classification, the region has a Cwa climate, humid subtropical, with hot and humid summers and cold and dry winters, with an annual average air temperature of 19.4 °C and average annual total rainfall of 1530 mm [16].

Additionally,  $\Psi_w$  (in MPa) was determined following Scholander et al. [17], using a Scholander pressure chamber (1000 PMS Instruments Plant Moisture). All measurements were made in fully expanded leaves of the 3rd or 4th pair from the tip of an actively growing branch (plagiotropic branch). In order to avoid any inhibitory effects of light or temperature on the leaf water potential, the measurements were conducted before dawn (between 04:30 and 05:30), at a mean temperature of 18 °C. Moreover, for the matter of this study, coffee plants were sampled in a 44.2 m<sup>2</sup> area at each 10 m.  $\Psi_w$  was evaluated for 17 dates, using the mean values of four replicates for the satellite images comparison.

**Table 1. Landsat-8/OLI configuration for each spectral band (Barsi et al., 2014).**

OLI Bands	Spectral Interval (nm)	Signal-To-Noise Ratio
B1	435–451	238
B2	452–512	364
B3	533–590	302
B4	636–673	227
B5	851–879	204
B6	1566–1651	265
B7	2107–2294	334

<https://doi.org/10.1371/journal.pone.0230013.t001>

Remote sensing data were obtained from Landsat-8 satellite imagery, Operational Land Imager (OLI). The Landsat-8 satellite was selected due to its spatial resolution and data availability close to the field campaigns. Launched in 2013, OLI sensor provides imagery with 30 m spatial resolution in the visible to shortwave infrared wavelengths (See Table 1), with a revisit time of 16 days [18]. This sensor shows similar characteristics when compared to other sensors from the Landsat program (i.e., Landsat-5 and Landsat-7) with more advanced radiometric and geometric quality.

The images were obtained free of charge via the United States Geological Survey (<https://earthexplorer.usgs.gov/>) for the path-row 218–75 in surface reflectance (Landsat 8 Surface Reflectance product–L8SR) [19]. L8SR uses an internal algorithm to provide the user with a product with atmospheric correction. The correction used in L8SR is based on the 6SV (Second Simulation of the Satellite Signal in the Solar Spectrum–Vector Version) [19,20] and several authors demonstrated the accuracy of such correction for different targets worldwide, such as vegetation [21,22] and water [23].

Images from the years 2014, 2015, 2016, and 2017 were selected for dates close to the field  $\Psi_w$  collection dates. The spectral bands used are in Table 2. To obtain the surface reflectance values, a pixel was selected in each of the field experiments: (i) Lavras with 21°13'40" S; 44°57'44" W; altitude 963 m and (ii) Santo Antônio do Amparo: 20°54'57" S; 44°51'13" W; altitude 1090 m. The band values 2, 3, 4, 5 and 6 were extracted in coordinates abovementioned. With the reflectance values, vegetation indices NDVI [24] and NDWI [25] were calculated using Eqs 1 and 2 for NDVI and NDWI, respectively.

$$\text{NDVI} = \frac{R_{850} - R_{640}}{R_{850} + R_{640}} \quad (1)$$

$$\text{NDWI} = \frac{R_{850} - R_{1600}}{R_{850} + R_{1600}} \quad (2)$$

Where  $R_{850}$ ,  $R_{640}$ , and  $R_{1600}$  are the reflectance at bands 5, 3 and 6 of OLI sensor with the subscript referring to the center wavelength of each spectral band. Moreover, precipitation

**Table 2. Regression models and coefficient of determination ( $R^2$ ).** Where B represents the satellite's spectral bands.

Model Name	Models	Pearson r	$R^2$
B2 <sub>Lin</sub>	$\Psi_w = 0.1266 - 33.1014 (B2)$	-0.85	0.71
B3 <sub>Lin</sub>	$\Psi_w = 0.5308 - 24.4544 (B3)$	-0.61	0.33
B4 <sub>Lin</sub>	$\Psi_w = 0.4577 - 24.9085 (B4)$	-0.84	0.68
B5 <sub>Lin</sub>	$\Psi_w = -2.038 + 3.891 (B5)$	0.57	0.28
B6 <sub>Lin</sub>	$\Psi_w = 1.473 - 9.955 (B6)$	-0.56	0.27
NDVI <sub>Lin</sub>	$\Psi_w = -4.329 + 4.806 (\text{NDVI})$	0.91	0.82
NDWI <sub>Lin</sub>	$\Psi_w = -1.455 + 2.375 (\text{NDWI})$	0.74	0.52
B2 <sub>Quad</sub>	$\Psi_w = -0.2065 - 10.9849 (B2) - 267.6433 (B2)^2$	-	0.71
B3 <sub>Quad</sub>	$\Psi_w = -3.135 + 107.559 (B3) - 1096.141 (B3)^2$	-	0.48
B4 <sub>Quad</sub>	$\Psi_w = -0.0988 + 2.5995 (B4) - 193.7306 (B4)^2$	-	0.69
B5 <sub>Quad</sub>	$\Psi_w = -6.825 + 29.639 (B5) - 32.893 (B5)^2$	-	0.36
B6 <sub>Quad</sub>	$\Psi_w = -0.8057 + 12.3297 (B6) - 53.3119 (B6)^2$	-	0.23
NDVI <sub>Quad</sub>	$\Psi_w = -8.712 + 17.325 (\text{NDVI}) - 8.739 (\text{NDVI})^2$	-	0.89
NDWI <sub>Quad</sub>	$\Psi_w = -1.865 + 5.539 (\text{NDWI}) - 4.693 (\text{NDWI})^2$	-	0.52

<https://doi.org/10.1371/journal.pone.0230013.t002>

data were obtained through a National Institute of Meteorology (INMET) meteorological station located in Lavras (-21.75° and -45.00°).

Table 2 shows the regression models and their respective determination coefficients for  $\Psi_w$  estimation using the spectral bands and the NDVI plant index. The quadratic models showed higher values for the coefficient of determination. For a study in vineyards in the Mediterranean using a field spectroradiometer, Serrano et al. (2010) obtained  $R^2 = 0.57$ . When performing the multivariate analysis, using the VIF selection, the explanatory variables that best fit the multivariate model were bands 2 and both vegetation indices (NDWI and NDVI), with VIF values lower than 5. Therefore, the proposed multivariate model was  $\Psi_w = -2.4877 - 13.753(B2) + 0.26402 * NDVI + 0.4254 * NDWI$ , which presented  $R^2 = 0.83$  ( $p \leq 0.05$ ;  $n = 17$ ).

### Statistical analysis and algorithm validation

The statistical relationships between  $\Psi_w$  and remote sensing data were obtained by the coefficient of determination ( $R^2$ ) analysis and linear, quadratic, and multivariate models—with variable selected using the Variance Inflation Method (VIF) from R Package [26]. VIF is a widely used tool to measure the degree of multicollinearity between two or more predictor variables [27]. To validate the models, Leave One Out Cross-Validation (LOOCV) technique was applied to all models [28]. LOOCV is a commonly used statistical method for small sample sizes that allow whole samples to be used in training and validation procedures [29,30]. At each step,  $n-1$  samples were used to train the model and another one is used for validation. This process is repeatedly executed until all sample pairs were validated ( $n = 18$  in this work). For each model, Mean Absolute Percentage Error (MAPE) (Eq 3), Root Mean Squared Error (RMSE) (Eq 4), determination coefficient ( $R^2$ ) and Pearson  $r$  coefficient were calculated.

$$MAPE = 100 * \frac{\sum_{i=1}^n \frac{|y_i - x_i|}{x_i}}{n} \quad (3)$$

$$RMSE = \sqrt{\frac{\sum_{i=1}^n (x_i - y_i)^2}{n}} \quad (4)$$

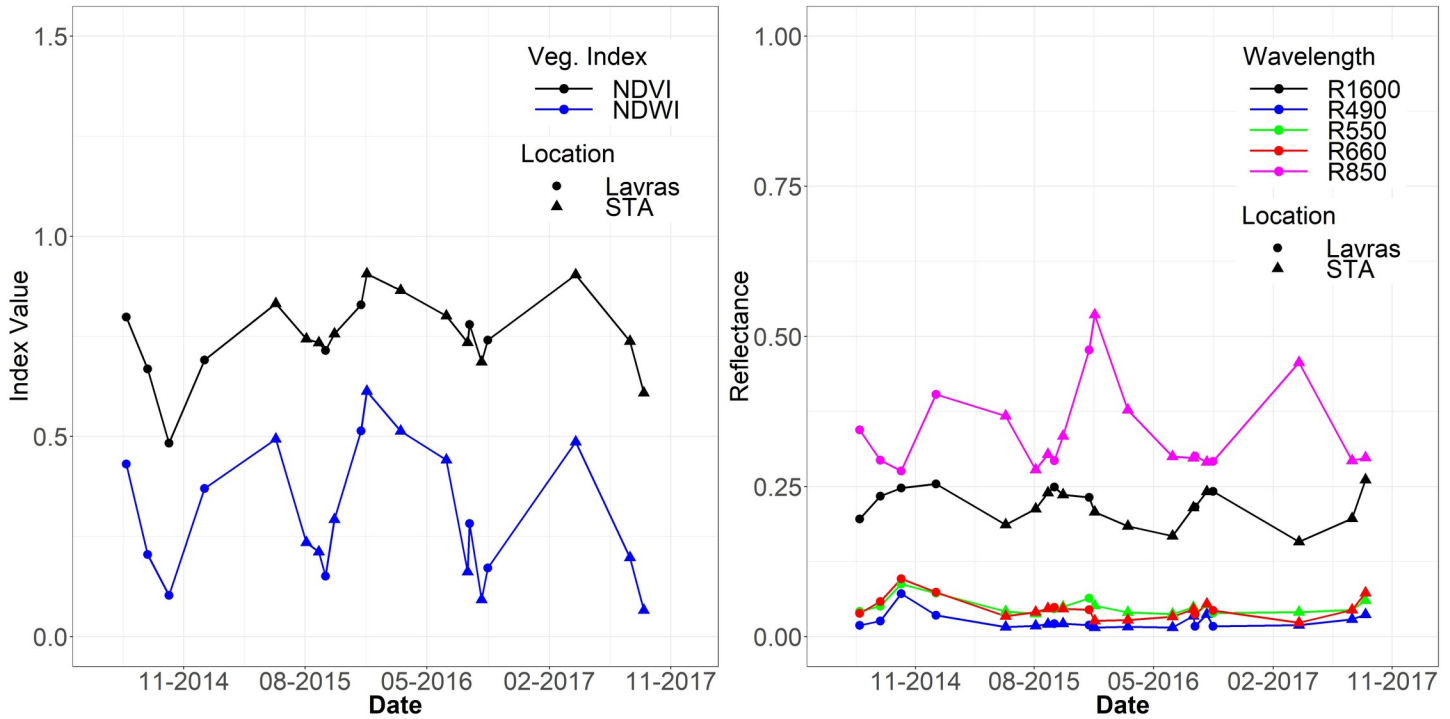
Where  $x_i$  is the field measured  $\Psi_w$  values, and  $y_i$  is the satellite estimated  $\Psi_w$  values for each station after the LOOCV. Therefore, after the algorithm validation, the one with the best results was applied to Landsat-8 imagery using a geographic information system (GIS) and  $\Psi_w$  was therefore calculated. To illustrate the spatialization of estimated  $\Psi_w$  values, a pilot area of approximately 13 km<sup>2</sup> was selected in Santo Antônio do Amparo, from September 2014 to July 2015.

## Results

### Variability of remote sensing, PH, and precipitation for the study area

Fig 2 shows the time-series of Landsat-8 reflectance values for both sites of Lavras and Santo Antônio do Amparo for NDVI and NDWI (Fig 2A), and bands 2, 3, 4, 5 and 6 (Fig 2B) for the dates of field surveys. Note that dates for Lavras and STA are referring to dates where  $\Psi_w$  was measured in each site. In the dates corresponding to the drought period in the region (August and September), the reflectance values in bands 2, 3, 4, and 6 increase, and the inverse occurs for band 5 and vegetation indices NDVI and NDWI. It is also important to note the variability of the intensity of NDVI values. For the drought season of 2014 (September 29), NDVI presented a value of 0.48, the lowest value in the analyzed time-series.

Fig 3 shows the monthly rainfall that occurred in the studied period, as well as the average normal rainfall for the region and the mean values of  $\Psi_w$ , measured in the field. The variation



**Fig 2.** Temporal variability of vegetation indices (A) and surface reflectance (B) for Lavras and Santo Antônio make Amparo points.

<https://doi.org/10.1371/journal.pone.0230013.g002>

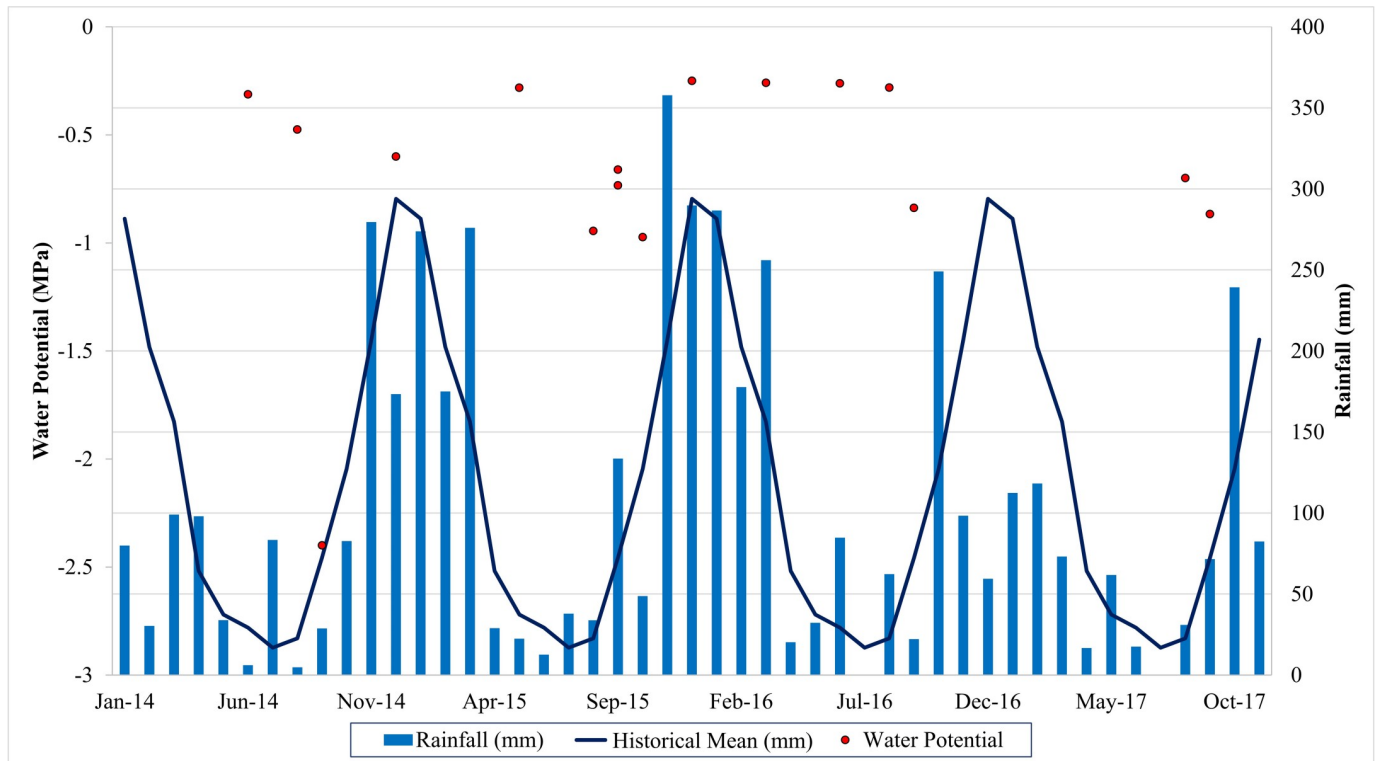
of  $\Psi_w$  values was from 0 up to -1 MPa, except for September 2014, when the value reached -2.4 MPa.  $\Psi_w$  values follow the observed for the vegetation indices and reflectances (Fig 2A and 2B), as the minimum  $\Psi_w$  was for the same date of minimum NDVI value. On the other dates,  $\Psi_w$  follows the tendency of the spectral response, being high in the rainy period and low at the end of the dry season.

Concerning the precipitation levels, the precipitation in 2014 was much lower than expected, according to the historical mean. The water potential is a crucial water relation parameter that describes the energy state of water; low  $\Psi_w$  is associated with the extent of plant dehydration [31]. Therefore, according to the values of  $\Psi_w$ , the region has favorable climatic conditions to maintain coffee hydration, but the occurrence of low rainfall in 2014 resulted in a moderate water deficit to the plants. Variations in leaf water status may cause alterations in photosynthetic pigment concentrations and photosynthetic activity, in turn, leading to changes in spectral reflectance properties [32].

### Leaf water potential algorithms

The best Pearson correlations were between the values of  $\Psi_w$  and the spectral bands of the visible B2 (R = -0.85), B3 (R = -0.61), and B4 (R = -0.84) (Table 2). There was a strong negative correlation indicating that for smaller  $\Psi_w$  values, a higher reflectance occurs in these bands. The results obtained for the bands of blue and red (bands 2 and 4, respectively), characterize a higher reflectance in the absorption bands of chlorophyll, indicating a smaller photosynthetically active area. Drought stress stimulates earlier leaf senescence, particularly in physiologically older leaves. Besides, this drought stress can decrease the net photosynthetic rate per unit leaf area. These decreases are strongly associated with stomatal factors, as coffee stomata are quite sensitive to both soil water availability and evaporative air demand [31].





**Fig 3. Variability of  $\Psi_w$  (MPa) values, total rainfall (mm), and average mean rainfall (mm), according to the meteorological station (Lavras, MG), from 2014 to 2017.**

<https://doi.org/10.1371/journal.pone.0230013.g003>

### LOOCV results and spatialization

Then, the models were applied to the LOOCV technique in order to validate the empirically developed algorithms. The results of the LOOCV were presented in Table 3. For most of the algorithms, the results were not accurate, with  $R^2$  values lower than 0.6 and MAPE and RMSE values high, indicating errors of up to 50% in the  $\Psi_w$  estimate (MAPE values higher than 50% were not shown in Table 3 for brevity).

The best result obtained for the LOOCV was for the Quadratic NDVI algorithm (NDVI<sub>Quad</sub>), with errors lower than 30%. Moreover, a good agreement between the field-measured  $\Psi_w$  and the predicted  $\Psi_w$  by OLI sensor ( $R^2 = 0.84$ , Pearson  $r = 0.92$ ) was observed. These

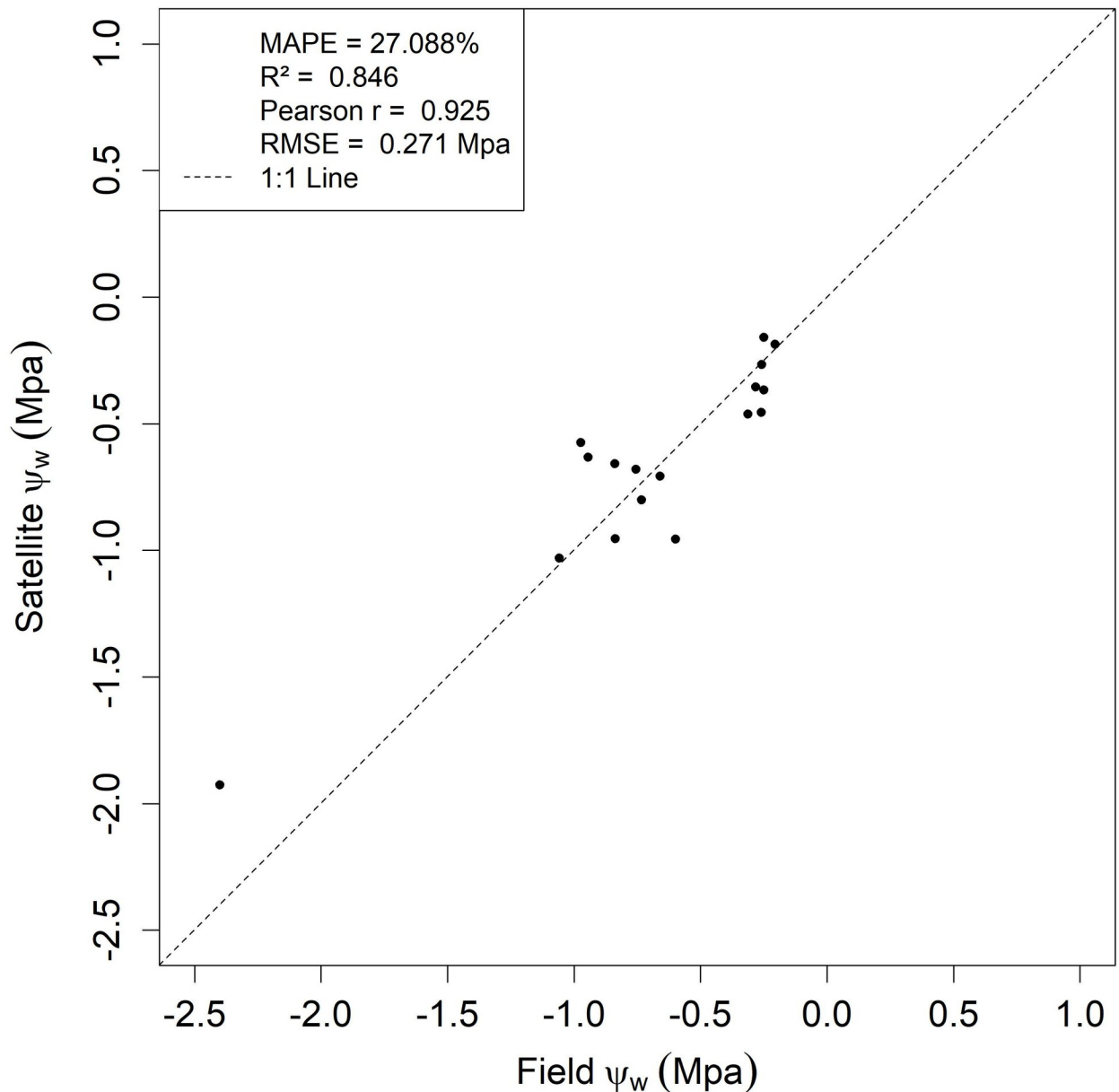
**Table 3. Statistical results obtained through the LOOCV.**

Model Name	MAPE (%)	$R^2$	Pearson $r$	RMSE (Mpa)
MV*	48.97	0.18	0.48	0.48
B4 <sub>Lin</sub>	44.63	0.39	0.66	0.39
NDVI <sub>Lin</sub>	45.23	0.67	0.83	0.29
NDWI <sub>Lin</sub>	37.18	0.34	0.62	0.41
B4 <sub>Quad</sub>	49.79	0.05	-0.14	0.65
NDVI <sub>Quad</sub>	<b>27.09</b>	<b>0.85</b>	<b>0.93</b>	<b>0.21</b>
NDWI <sub>Quad</sub>	31.33	0.24	0.54	0.46

Values in bold indicate the best results for each statistical metric.

\*Multivariate Model

<https://doi.org/10.1371/journal.pone.0230013.t003>



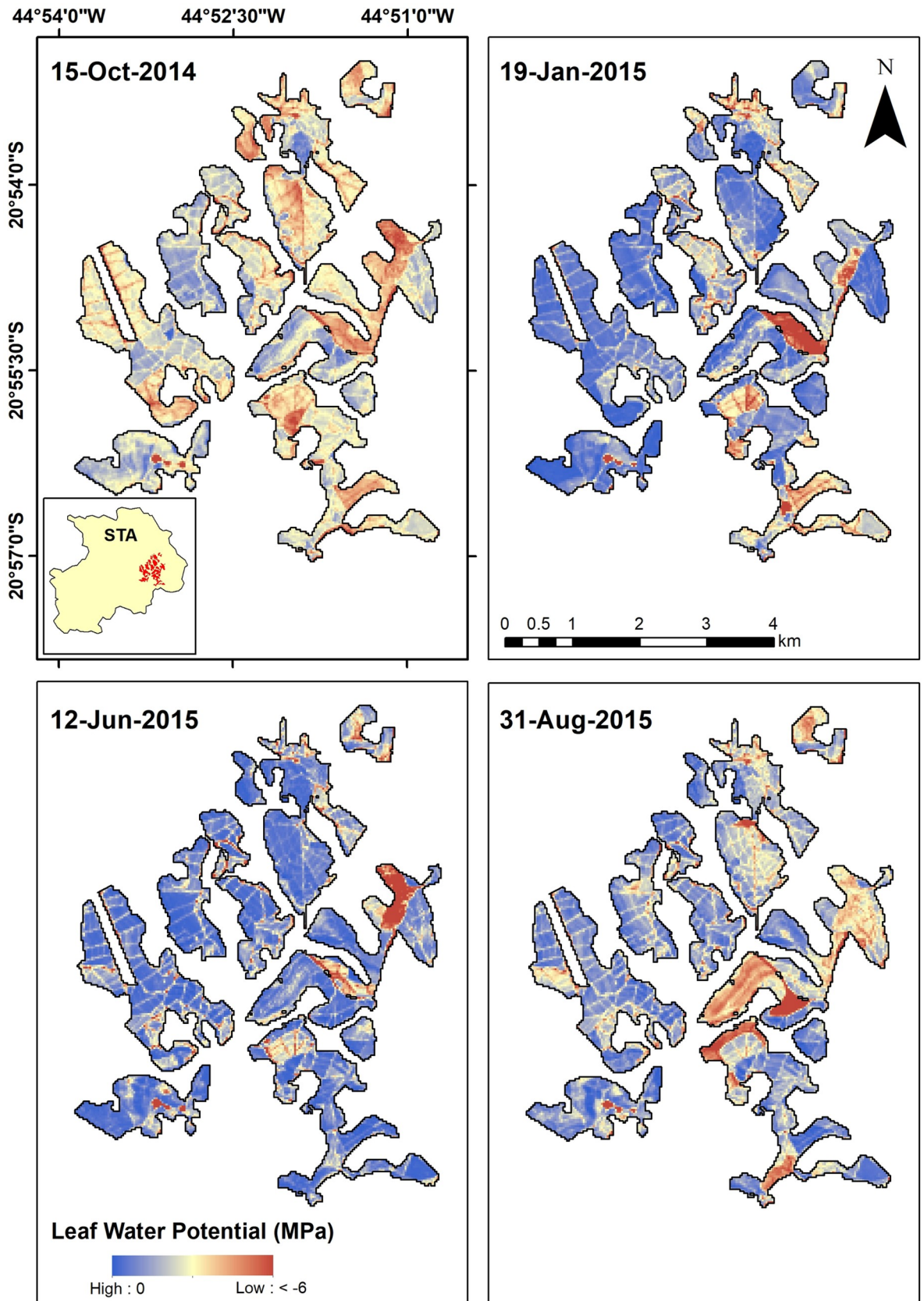
**Fig 4. LOOCV results for the NDVI<sub>Quad</sub> algorithm.** The upper left box refers to MAPE,  $R^2$ , Pearson  $r$ , and RMSE for the validation using LOOCV.

<https://doi.org/10.1371/journal.pone.0230013.g004>

results are in agreement with the exploratory analysis (See Table 3), in which NDVI<sub>Quad</sub> was the best regression to estimate  $\Psi_w$ . Fig 4 shows the results of the LOOCV using the NDVI<sub>Quad</sub> algorithm, with the satellite predicted  $\Psi_w$  and the values obtained in the field.

Thus, with the best results for the NDVI<sub>Quad</sub> model, it was inserted into the geographic information system (GIS) and the values of  $\Psi_w$  were estimated from Landsat-8 OLI images between September 2014 and July 2015, corresponding to a dry and rainy period, respectively. Fig 5 shows the map of estimated  $\Psi_w$  values in an area representative of the study region. It was estimated that, during the dry season (September/2014), the mean  $\Psi_w$  value was  $-0.91 \pm 0.35$  MPa. For January 2015, as precipitation increases, the mean  $\Psi_w$  was  $-0.70 \pm 0.29$  MPa. The increase in  $\Psi_w$  values was also observed until June 2015, with mean estimated  $\Psi_w$  of  $-0.50 \pm 0.25$  MPa.





**Fig 5.  $\Psi_w$  estimated (MPa) between September 2014 and July 2015, in an area representative of the study region, in Santo Antônio do Amparo.**

<https://doi.org/10.1371/journal.pone.0230013.g005>

With the end of the rainy season, mean  $\Psi_w$  starts to decrease again (mean values of  $-0.61 \pm 0.25$  MPa). Furthermore, as orbital remote sensing provides a synoptic view of land areas, the spatial variability of  $\Psi_w$  can be beneficial for planning coffee management.

## Discussions

The currently widely used method to assess plant drought and water status is the pressure chamber. However, this method has the limitations of being destructive, point-based, and user-dependent, which restricts large areas of monitoring. In this work, we provided a Landsat-8/OLI-based  $\Psi_w$  algorithm using NDVI to predict  $\Psi_w$  with reliable accuracy (MAPE < 30%,  $R^2 > 0.85$ , RMSE < 0.21 Mpa). Therefore, it was possible to apply the algorithm and obtain a synoptic view of an experiment area, which could contribute to cost reduction in coffee water status management.

The use of NDVI as an indicator of drought vegetation stress and soil moisture was already reported by several authors [2,9,10,12] as NDVI provides a general measurement of vegetation state and health and has been used for accessing drought status since the 1970s when this index was proposed by Rouse [33]. However, there is also a difficulty in monitoring water stress using vegetation indices as this response is observed when notable damage to the culture has already occurred [10].

When the plant is submitted to a water stress condition, NDVI values tend to decrease as water conditions alter the biophysical conditions in the leaves. Despite near-infrared and red bands not being directly correlated with the water content, they are linked to chlorophyll and other biophysical parameters such as aboveground net primary production [34], green leaf biomass and leaf photosynthetic activity [35] and these variables are linked to water stress [36]. Gu et al. [37] found a high correlation ( $r = 0.73$ ) between fractional water index (FWI) and both NDVI and NDWI for sites surrounded by relatively homogeneous vegetation with silt loam soils at Oklahoma, USA. Furthermore, Mbatha and Xulu (2018) also demonstrate the applicability of NDVI to monitor the impact of intense drought in South Africa due to El Niño effects. The results obtained for the quadratic NDVI model in this work were better than those obtained by Ramoelo et al. (2015) and better than those obtained by Rallo et al. (2014), with  $R^2 = 0.36$  and RMSE of 0.44 MPa, and Cotrozzi et al. (2017), with  $R^2 = 0.65$  and RMSE of 0.51 MPa, using a field spectroradiometer.

## Conclusions

In this work, we provided an empirical algorithm for estimate Leaf Water Potential ( $\Psi_w$ ) using Landsat-8 surface reflectance and vegetation indices data for Coffee Arabica areas in Minas Gerais state, Brazil. From the validation, a quadratic NDVI algorithm presented the best result for  $\Psi_w$  estimative, with Mean Absolute Percentage Error (MAPE) of 27.09% and an  $R^2$  of 0,85, being, therefore, an option to estimate  $\Psi_w$  of coffee areas from the surface reflectance obtained from the Landsat-8 satellite OLI sensor. The spatialization of the estimated  $\Psi_w$  values in the region is a technology that can enable the satellite monitoring of water conditions of coffee plants to establish appropriate practices, such as irrigation economics, pest and disease control, and fertilization management, allowing environmental and economic sustainability of coffee plantations in the largest coffee region of Brazil.

## Supporting information

**S1 Data.**  
(XLSX)

## Acknowledgments

The authors would like to thank CNPq, FAPEMIG, CAPES, Consórcio Pesquisa Café.

## Author Contributions

**Conceptualization:** Vânia Aparecida Silva.

**Data curation:** Daniel Andrade Maciel, Vânia Aparecida Silva, Helena Maria Ramos Alves, Vanessa Cristina Oliveira de Souza, Helbert Rezende de Oliveira Silveira, Mayara Fontes Dantas.

**Formal analysis:** Daniel Andrade Maciel, Helena Maria Ramos Alves, Vanessa Cristina Oliveira de Souza, Mayara Fontes Dantas, Ana Flávia de Freitas.

**Investigation:** Meline Oliveira Santos, Helbert Rezende de Oliveira Silveira, Ana Flávia de Freitas.

**Methodology:** Vânia Aparecida Silva, Vanessa Cristina Oliveira de Souza, Meline Oliveira Santos, Helbert Rezende de Oliveira Silveira, Mayara Fontes Dantas.

**Project administration:** Vânia Aparecida Silva, Margarete Marin Lordelo Volpato.

**Resources:** João Paulo Rodrigues Alves de Barbosa.

**Software:** Ana Flávia de Freitas.

**Validation:** Daniel Andrade Maciel, Meline Oliveira Santos, Helbert Rezende de Oliveira Silveira, Gladyston Rodrigues Carvalho.

**Visualization:** Daniel Andrade Maciel, Helena Maria Ramos Alves, João Paulo Rodrigues Alves de Barbosa, Gladyston Rodrigues Carvalho.

**Writing – original draft:** Gladyston Rodrigues Carvalho, Jacqueline Oliveira dos Santos.

**Writing – review & editing:** Jacqueline Oliveira dos Santos.

## References

1. Lu J, Carbone GJ, Gao P. Mapping the agricultural drought based on the long-term AVHRR NDVI and North American Regional Reanalysis (NARR) in the United States, 1981–2013. *Appl Geogr.* 2019; 104: 10–20. <https://doi.org/10.1016/j.apgeog.2019.01.005>
2. Mbatha N, Xulu S. Time Series Analysis of MODIS-Derived NDVI for the Hluhluwe-Imfolozi Park, South Africa: Impact of Recent Intense Drought. *Climate.* 2018; 6: 95. <https://doi.org/10.3390/cli6040095>
3. Ozelkan E, Chen G, Ustundag BB. Multiscale object-based drought monitoring and comparison in rainfed and irrigated agriculture from Landsat 8 OLI imagery. *Int J Appl Earth Obs Geoinf.* 2016; 44: 159–170. <https://doi.org/10.1016/j.jag.2015.08.003>
4. Nichol JE, Abbas S. Integration of remote sensing datasets for local scale assessment and prediction of drought. *Sci Total Environ.* 2015; 505: 503–507. <https://doi.org/10.1016/j.scitotenv.2014.09.099> PMID: 25461052
5. Claverie M, Ju J, Masek JG, Dungan JL, Vermote EF, Roger J, et al. The Harmonized Landsat and Sentinel-2 surface reflectance data set. *Remote Sens Environ.* 2018; 219: 145–161. <https://doi.org/10.1016/j.rse.2018.09.002>

6. Ramoelo A, Dziki S, Van Deventer H, Maherry A, Cho MA, Gush M. Potential to monitor plant stress using remote sensing tools. *J Arid Environ.* 2015; 113: 134–144. <https://doi.org/10.1016/j.jaridenv.2014.09.003>
7. Chemura A, Mutanga O, Dube T. Remote sensing leaf water stress in coffee (*Coffea arabica*) using secondary effects of water absorption and random forests. *Phys Chem Earth.* 2017; 100: 317–324. <https://doi.org/10.1016/j.pce.2017.02.011>
8. Junges AH, Fontana DC, Anzanello R, Bremm C. Normalized difference vegetation index obtained by ground-based remote sensing to characterize vine cycle in Rio Grande do Sul, Brazil. *Ciência e Agroecologia.* 2017; 41: 543–553. doi:<https://doi.org/10.1590/1413-70542017415049016>.
9. Aguilar C, Zinnert JC, Polo MJ, Young DR. NDVI as an indicator for changes in water availability to woody vegetation. *Ecol Indic.* 2012; 23: 290–300. <https://doi.org/10.1016/j.ecolind.2012.04.008>
10. Cunha APM, Alvalá RC, Nobre CA, Carvalho MA. Monitoring vegetative drought dynamics in the Brazilian semiarid region. *Agric For Meteorol.* 2015; 214–215: 494–505. <https://doi.org/10.1016/j.agrformet.2015.09.010>
11. Damatta FM, Ramalho JDC. Impacts of drought and temperature stress on coffee physiology and production: a review. *Braz J Plant Physiol.* 2006; 18: 55–81. <https://doi.org/10.1590/S1677-04202006000100006>
12. Nanzad L, Zhang J, Tuvdendorj B, Nabil M, Zhang S, Bai Y. NDVI anomaly for drought monitoring and its correlation with climate factors over Mongolia from 2000 to 2016. *J Arid Environ.* 2019; 164: 69–77. <https://doi.org/10.1016/j.jaridenv.2019.01.019>
13. Pu R, Ge S, Kelly NM, Gong P. Spectral absorption features as indicators of water status in coast live oak (*Quercus agrifolia*) leaves. *Int J Remote Sens.* 2003; 24: 1799–1810. <https://doi.org/10.1080/01431160210155965>
14. Fensholt R, Nielsen TT, Stisen S. Evaluation of AVHRR PAL and GIMMS 10-day composite NDVI time series products using SPOT-4 vegetation data for the African continent. *Int J Remote Sens.* 2006; 27: 2719–2733.
15. Rallo G, Minacapilli M, Ciraolo G, Ed S. Detecting crop water status in mature olive groves using vegetation spectral measurements. *Biosyst Eng.* 2014; 128: 52–68. <https://doi.org/10.1016/j.biosystemseng.2014.08.012>
16. Köppen, Wladimir; Geiger R. *Handbuch der Klimatologie: Das geographische System der Klimate.* Verlag von Gebrüder Borntraeger. 1936. <https://doi.org/10.3354/cr01204>
17. Scholander PF, Hammel HT, Hemmingsen EA, Bradstreet ED. HYDROSTATIC PRESSURE AND OSMOTIC POTENTIAL IN LEAVES OF MANGROVES AND SOME OTHER PLANTS. *Proc Natl Acad Sci.* 2006. <https://doi.org/10.1073/pnas.52.1.119> PMID: 16591185
18. Wulder MA, Loveland TR, Roy DP, Crawford CJ, Masek JG, Woodcock CE, et al. Current status of Landsat program, science, and applications. *Remote Sens Environ.* 2019; 225: 127–147. <https://doi.org/10.1016/j.rse.2019.02.015>
19. Vermote E, Justice C, Claverie M, Franch B. Preliminary analysis of the performance of the Landsat 8/OLI land surface reflectance product. *Remote Sens Environ.* 2016; 185: 46–56. <https://doi.org/10.1016/j.rse.2016.04.008> PMID: 32020955
20. Vermote EF, Tanré D, Deuzé JL, Herman M, Morcrette JJ. Second Simulation of the Satellite Signal in the Solar Spectrum (6S). 6S User Guide Version 2. Appendix III: Description of the subroutines. *IEEE Trans Geosci Remote Sens.* 1997; 35: 675–686. <https://doi.org/10.1109/36.581987>
21. Doxani G, Vermote E, Roger JC, Gascon F, Adriaensen S, Frantz D, et al. Atmospheric correction inter-comparison exercise. *Remote Sens.* 2018; 10: 1–18. <https://doi.org/10.3390/rs10020352>
22. Vuolo F, Mattiuzzi M, Atzberger C. Comparison of the Landsat Surface Reflectance Climate Data Record (CDR) and manually atmospherically corrected data in a semi-arid European study area. *Int J Appl Earth Obs Geoinf.* 2015; 42: 1–10. <https://doi.org/10.1016/j.jag.2015.05.003>
23. Maciel DA, Novo E, Sander de Carvalho L, Barbosa C, Flores Júnior R, de Lucia Lobo F, et al. Retrieving Total and Inorganic Suspended Sediments in Amazon Floodplain Lakes: A Multisensor Approach. *Remote Sens.* 2019; 11: 1744. <https://doi.org/10.3390/rs11151744>
24. Rouse J Jr, Haas RH, Schell JA, Deering DW. Monitoring vegetation systems in the Great Plains with ERTS. 1974.
25. Gao B- C. NDWI—A normalized difference water index for remote sensing of vegetation liquid water from space. *Remote Sens Environ.* 1996; 58: 257–266.
26. Fox J, Weisberg S. *An {R} Companion to Applied Regression.* Second. Thousand Oaks {CA}: Sage; 2011. Available: <http://socserv.socsci.mcmaster.ca/jfox/Books/Companion>

27. Thompson CG, Kim RS, Aloe AM, Becker BJ. Extracting the Variance Inflation Factor and Other Multicollinearity Diagnostics from Typical Regression Results. *Basic Appl Soc Psych*. 2017; 39: 81–90. <https://doi.org/10.1080/01973533.2016.1277529>
28. Stone M. Cross-validated choice and assessment of statistical predictions. *J R Stat Soc Ser B*. 1974; 36: 111–133.
29. Davidson A, Wang S, Wilmshurst J. Remote sensing of grassland–shrubland vegetation water content in the shortwave domain. *Remote Sens Grassland–shrubl Veg water content shortwave domain*. 2006; 8: 225–236. <https://doi.org/10.1016/j.jag.2005.10.002>
30. Goutte C. Note on free lunches and cross-validation. *Neural Comput*. 1997; 9: 1245–1249.
31. Damatta FM, Avila RT, Cardoso AA, Martins SCV, Ramalho JC. Physiological and Agronomic Performance of the Coffee Crop in the Context of Climate Change and Global Warming: A Review. *Journal of Agricultural and Food Chemistry*. 2018. <https://doi.org/10.1021/acs.jafc.7b04537> PMID: 29517900
32. Grace J, Nichol C, Disney M, Lewis P, Quaife T, Bowyer P. Can we measure terrestrial photosynthesis from space directly, using spectral reflectance and fluorescence? *Glob Chang Biol*. 2007; 13: 1484–1497. <https://doi.org/10.1111/j.1365-2486.2007.01352.x>
33. Rouse JW, Hass RH, Schell JA, Deering DW, Harlan JC. Monitoring the vernal advancement and retrogradation (green wave effect) of natural vegetation. Final Report, RSC 1978–4, Texas A M Univ Coll Station Texas. 1974.
34. Paruelo JM, Epstein HE, Lauenroth WK, Burke IC. ANPP estimates from NDVI for the central grassland region of the United States. *Ecology*. 1997; 78: 953–958.
35. Curran P. Multispectral photographic remote sensing of vegetation amount and productivity. 14 International Symposium on Remote Sensing of Environment San Jose (Costa Rica) 23–30 Apr 1980. 1980.
36. Joiner J, Yoshida Y, Anderson M, Holmes T, Hain C, Reichle R, et al. Global relationships among traditional reflectance vegetation indices (NDVI and NDII), evapotranspiration (ET), and soil moisture variability on weekly timescales. *Remote Sens Environ*. 2018; 219: 339–352. <https://doi.org/10.1016/j.rse.2018.10.020> PMID: 31217640
37. Gu Y, Hunt E, Wardlow B, Basara JB, Brown JF, Verdin JP. Evaluation of MODIS NDVI and NDWI for vegetation drought monitoring using Oklahoma Mesonet soil moisture data. *Geophys Res Lett*. 2008; 35: 1–5. <https://doi.org/10.1029/2008GL035772>